

# Two Dimensional Poynting Flux Dominated Flow onto a Schwarzschild Black Hole

Hyun Kyu Lee\* and Jaehong Park†

*Department of Physics Hanyang University, Seoul 133-791, Korea*

(Dated: January 17, 2022)

We discuss the dynamics of the accretion flow onto a black hole driven by Poynting flux in a simplified model of a two-dimensional accretion disk. In this simplified model, the condition of the stationary accretion flow is found to impose a nontrivial constraint on the magnetic field configuration. The effect of the magnetic field on the accretion flow is discussed in detail using the paraboloidal and hyperboloidal type configuration for the poloidal structure suggested by Blandford in 1976. It is demonstrated explicitly that the angular velocity of the disk,  $\Omega_D$ , deviates from the Keplerian angular velocity. The angular velocity of the rigidly-rotating magnetic surface,  $\Omega_F$ , does not have to be the same as the angular velocity of the disk for the paraboloidal type configuration. But for the hyperboloidal type configuration, it is found that we can set  $\Omega_F = \Omega_D$ , which corresponds to an accretion disk of perfect conductor. We discuss the numerical solutions of the stream equation for stationary accretion flow in the Schwarzschild background using a paraboloidal type configuration. The dynamics of the accretion disk is found to depend strongly on the ratio of the accretion rate to the magnetic field strength.

PACS numbers: 97.10.Gz, 97.60.Lf

## I. INTRODUCTION

To describe the powerful and highly collimated astrophysical jets observed in AGN and quasars, Poynting flux model has been suggested long time ago [1, 2] and many interesting works have been developed. One of the characteristics of Poynting flux is that it carries very little baryonic component compared to the hydrodynamic flow. Recently this property of Poynting flux is found to be consistent with the required property for powering GRB[3]. And the Poynting flux in a system of black hole-accretion disk has also been studied in connection with the gamma ray bursts[4, 5, 6] and it is found that the evolution of the system is largely depend on the Poynting outflow from the disk[7, 8].

The configuration of the ordered magnetic field around the accretion disk, which is responsible for the Poynting flux, has been discussed both in analytical and numerical studies. For the strong enough electromagnetic field around the compact object, the force-free magnetosphere can be established. In the non-relativistic formulation, Blandford[2] suggested an axisymmetric and stationary solution for the Poynting outflow, assuming a force-free magnetosphere surrounding an accretion disk. The poloidal field configuration for a black hole in a force-free magnetosphere has been discussed recently by Ghosh[9] in the relativistic formulation using Grad-Shfranov equation. The developments of the ordered magnetic field in the disk and the Poynting outflow from the disk have been studied numerically by many authors[10, 11, 12]. Recently Ustyugova et al.[13] performed an axisymmetric magneto-hydrodynamical simulation to show that the

quasi-stationary and approximately force-free Poynting jet from the inner part of the accretion disk is possible.

In studying the accretion flow, it is also important to know the dynamics of the accretion disk influenced by the magnetic field. The energy and angular momentum carried out by the Poynting flux are determined essentially by the torque and the angular velocity of the magnetic surface  $\Omega_F$ , which depends strongly on the disk dynamics subjected to the magnetic field. We adopt a simplified two-dimensional accretion disk model[14] embedded in a stationary, axisymmetric and force-free magnetosphere. To see the magnetic effect transparently it is also assumed that there is no viscous stress tensor in the disk and there is no radiative transfer from the disk in this model.

The state of an accretion flow is governed by a set of equations obtained from the conservation of stress-energy tensor[14] and the force-free magnetosphere with the current configuration is determined by the Grad-Shafranov equation. The two sets of equations are not completely independent to each other because they are coupled at the disk on the equatorial plane. Hence the variables in the Grad-Shfranov equations, the stream function  $\Psi$ , the current potential  $I$  and  $\Omega_F$  are constrained by the accretion equations. In other words, the accretion equations provide a kind of boundary values of  $\Psi$ ,  $I$  and  $\Omega_F$  which cannot be determined by Grad-Shafranov equation alone. It also impose a nontrivial constraint on the configuration type of the magnetic field. For example, it is found that the hyperboloidal configuration suggested by Blandford in 1976[2] is consistent with an accretion disk of perfect conductor, that is  $\Omega_F = \Omega_D$ , for the stationary accretion flow, whereas for the paraboloidal type configuration  $\Omega_F$  does not have to be the same as  $\Omega_D$ .

In section 2, we describe the simplified two-dimensional accretion disk model dominated by Poynting flux in a force-free magnetosphere. The system is governed by four

\*Electronic address: hkleee@hepth.hanyang.ac.kr; Also at APCTP, Pohang 790-784, Korea

†Electronic address: jaehong@ihanyang.ac.kr

basic equations: three accretion equations and the Grad-Shafranov equation in the Schwarzschild background. In section 3, numerical analysis of the accretion flow and the field configuration of paraboloidal type are discussed in detail for two cases of lower and higher accretion rates. The results are summarized and discussed in section 4.

## II. TWO DIMENSIONAL ACCRETION DISK IN FORCE-FREE MAGNETOSPHERE

In this work, a black hole-accretion disk system is supposed to be surrounded by the ordered electromagnetic field, which is determined by the electric charge and current distributions as a solution of the inhomogeneous Maxwell equation:

$$F^{\mu\nu}_{;\nu} = 4\pi J^\mu \quad (1)$$

where  $J^\mu$  are the  $\mu$ -th component of the bulk electromagnetic current density. The boundary values for the field configuration are responsible to the surface current densities on the horizon and/or on the accretion disk. It is a kind of boundary value problem[15], which can be described by introducing appropriate surface current densities,  $j^\mu$ , defined on the surface such that the total conserved current density, is given by

$$\mathcal{J}^\mu = J^\mu + j^\mu. \quad (2)$$

Using the current conservation,

$$\mathcal{J}^\mu_{;\mu} = 0, \quad (3)$$

one can identify the surface current density when provided with the geometry of the surface.

The horizon of a black hole is a mathematically well defined surface, on which the appropriate surface current density has been studied in depth[16]. On the other hand, the surface of the physical accretion disk is not expected to have any sharp boundary and various shapes have been suggested depending on the properties of accretion flow. In this work, however, we assume a simplified accretion disk, which is vertically squeezed down to the equatorial plane, a two-dimensional accretion disk. Then we can associate the surface current density in a simple way,

$$j^\mu = \frac{1}{4\pi}(F_+^{\theta\mu} - F_-^{\theta\mu})\delta(\theta - \pi/2), \quad (4)$$

which are nothing but Gauss' law and Ampere's law as given by

$$\sigma_e = -\frac{1}{4\pi}(E_+^\theta - E_-^\theta), \quad (5)$$

$$K^{\hat{r}} = -\frac{1}{4\pi}(B_+^{\hat{\phi}} - B_-^{\hat{\phi}}), \quad K^{\hat{\phi}} = \frac{1}{4\pi}(B_+^{\hat{r}} - B_-^{\hat{r}}), \quad (6)$$

where  $\sigma_e$  and  $K^i$  are surface charge and surface current density (spatial) respectively and  $+/-$  denote the upper/lower hemisphere.

### A. Accretion equations

The dynamics of an accretion flow is determined by the conservation equation of the stress-energy tensor:

$$T^{\mu\nu}_{;\mu} = 0. \quad (7)$$

The stress-energy tensor is decomposed into two parts, the matter ( $T_m^{\mu\nu}$ ) and the electromagnetic ( $T_{EM}^{\mu\nu}$ ) parts:

$$T^{\mu\nu} = T_m^{\mu\nu} + T_{EM}^{\mu\nu}. \quad (8)$$

The electromagnetic part is given by

$$T_{EM}^{\mu\nu} = \frac{1}{4\pi} \left( F^\mu_\rho F^{\nu\rho} - \frac{1}{4} g^{\mu\nu} F_{\rho\sigma} F^{\rho\sigma} \right). \quad (9)$$

In general the stress-energy tensor for the accretion disk is determined by mass density, internal energy, pressure, viscosity, radiative transfer and etc.[17]. Since we are interested in the accretion dominated by the Poynting flux, the two-dimensional accretion disk is assumed to be non-viscous, cool, and non-radiative such that the matter part is given by

$$T_m^{\mu\nu} = \rho_m u^\mu u^\nu, \quad (10)$$

where  $\rho_m$  is the rest-mass density and  $u^\mu$  is the four velocity of the accreting matter.

From the conservation of stress-energy tensor, one can obtain[14]

$$(\partial_r u_0) \dot{M}_+ + 2\pi r K^{\hat{r}} (-\alpha E^{\hat{r}} + \beta \varpi B^{\hat{\theta}}) = 0, \quad (11)$$

$$(\partial_r u_\phi) \dot{M}_+ + 2\pi r K^{\hat{r}} \varpi B^{\hat{\theta}} = 0, \quad (12)$$

$$\begin{aligned} & \frac{\dot{M}_+}{2\pi r^2} g^{rr} \frac{u^0}{u^r} (\partial_r u_\phi) \left[ \Omega_D + \frac{\partial_r u_0}{\partial_r u_\phi} \right] \\ & - \frac{\sqrt{\Delta}}{r^2} (\sigma_e E^{\hat{r}} - K^{\hat{\phi}} B^{\hat{\theta}}) = 0. \end{aligned} \quad (13)$$

where the angular velocity of the disk is given by  $\Omega_D = u^{\hat{\phi}}/u^0$  and the mass accretion rate is given by

$$\dot{M}_+ = -2\pi r \sigma_m u^r. \quad (14)$$

Eq.(11) and (12) correspond to the energy and angular momentum conservation respectively in the stationary and axisymmetric setting in this work. One can see that the accretion is determined by the Poynting flux. The last equation is obtained from the radial component which essentially determines the orbital motion of the disk. Since  $u^\theta = 0$ , the  $\theta$ -component of the conservation equation does not contribute to the accretion flow. In the absence of external fields, the angular velocity is determined as

$$\Omega_D = -\frac{\partial_r u_0}{\partial_r u_\phi}, \quad (15)$$

which is one of the characteristics of the Keplerian orbit. Hence deviations of  $\Omega_D$  from the Keplerian one is naturally expected in the Poynting flux dominated accretion

disk. One of the purposes of this work is to see how it depends on the magnetic field.

In the force-free limit[18],

$$F_{\mu\nu}J^\nu = 0, \quad (16)$$

we get

$$\vec{E} = -\frac{\bar{\omega}}{\alpha}\Omega_F e_{\hat{\phi}} \times \vec{B}^p, \quad (17)$$

in the Schwarzschild background.  $\Omega_F$  is the angular velocity of the magnetic surface which rotates rigidly in an axisymmetric and stationary state [16]. Then the accretion equations driven by the Poynting flux can be rewritten as

$$(\partial_r u_0)\dot{M}_+ + r\varpi\Omega_F B^{\hat{\phi}}B^{\hat{\theta}} = 0, \quad (18)$$

$$(\partial_r u_\phi)\dot{M}_+ - r\varpi B^{\hat{\phi}}B^{\hat{\theta}} = 0, \quad (19)$$

$$\begin{aligned} & \frac{\dot{M}_+}{2\pi r^2} g^{rr} \frac{u_0}{u_r} (\partial_r u_\phi) \left[ \Omega_D + \frac{\partial_r u_0}{\partial_r u_\phi} \right] \\ & - \frac{\sqrt{\Delta}}{2\pi r^2} B^{\hat{r}} B^{\hat{\theta}} \left( \frac{\varpi^2}{\alpha^2} \Omega_F^2 - 1 \right) = 0. \end{aligned} \quad (20)$$

From eq.(18) and (19), one obtains an interesting relation

$$\frac{\partial_r u_0}{\partial_r u_\phi} = -\Omega_F. \quad (21)$$

which has no explicit dependence on the field configuration. It seems to imply that  $\Omega_F$  is determined essentially by the dynamics of the disk. However one should note that the dynamics itself is governed not only by the gravity but also by the electromagnetic field as well.

### B. Stream equation

The configuration of the ordered magnetic field around the accretion disk has been discussed both in analytical and numerical studies. The developments of the ordered magnetic field in the disk and the Poynting outflow from the disk have been studied numerically by many

authors[10, 11, 12]. For the strong enough electromagnetic field around the compact object, the force-free magnetosphere can be established. In the non-relativistic formulation, Blandford[2] suggested an axisymmetric and stationary electromagnetic field configuration around an accretion disk on the equatorial plane. The poloidal field configuration for a black hole is known to satisfy a second order elliptical differential equation called Grad-Shafranov equation[19] or a stream equation[20] for the stream function  $\Psi$  and current  $I$ . The poloidal and toroidal components of the magnetic field can be written in terms of  $\Psi$  and  $I$  respectively:

$$\begin{aligned} \vec{B}^P &= \frac{1}{2\pi\varpi} \nabla\Psi \times e_{\hat{\phi}}, \\ B^{\hat{\phi}} &= -\frac{2I}{\varpi\alpha}. \end{aligned} \quad (22)$$

Possible types of solutions in a force-free magnetosphere has been discussed recently in the relativistic formulation[9, 21].

In a flat background, the stream equation becomes simpler one given by

$$\begin{aligned} & \partial_r^2 \Psi + \frac{\sin\theta}{r^2} \partial_\theta \left( \frac{1}{\sin\theta} \partial_\theta \Psi \right) - \Omega_F \sin^2 \theta \partial_r (r^2 \Omega_F \partial_r \Psi) \\ & - \Omega_F \sin \theta \partial_\theta (\sin \theta \Omega_F \partial_\theta \Psi) = -16\pi^2 I \frac{dI}{d\Psi} \end{aligned} \quad (23)$$

Blandford[2] suggested two types of solution of eq.(23) depending on the types of surface, where magnetic field lines rotating with angular velocity  $\Omega_F$  lie on. In a upper hemisphere, the magnetic field of paraboloidal type cutting the disk on the equatorial plane is given by

$$\begin{aligned} B^{\hat{r}} &= \frac{C}{2r\{1 + \Omega_F^2 r^2 (1 - \cos\theta)^2\}^{1/2}}, \\ B^{\hat{\theta}} &= \frac{-C(1 - \cos\theta)}{2r \sin\theta \{1 + \Omega_F^2 r^2 (1 - \cos\theta)^2\}^{1/2}}, \\ B^{\hat{\phi}} &= \frac{-C\Omega_F(1 - \cos\theta)}{\sin\theta \{1 + \Omega_F^2 r^2 (1 - \cos\theta)^2\}^{1/2}}, \end{aligned} \quad (24)$$

and the solution of hyperboloidal type is given by

$$\begin{aligned}
B^{\hat{r}} &= \frac{B_0 R^2 (1 - \cos \theta)^2}{\{\sin^2 \theta R^2 - r^2 (1 - \cos \theta)^4\} \{R^2 - \Omega_F^2 r^4 (1 - \cos \theta)^4\}^{1/2}} \\
&\times \left[ (1 - \cos \theta) \{\sin^2 \theta - (1 - \cos \theta)^2\}^{1/2} + \{R^2 - r^2 (1 - \cos \theta)^2\}^{1/2} \cos \theta \right] \\
B^{\hat{\theta}} &= \frac{B_0 R^2 (1 - \cos \theta)^2}{\{\sin^2 \theta R^2 - r^2 (1 - \cos \theta)^4\} \{R^2 - \Omega_F^2 r^4 (1 - \cos \theta)^4\}^{1/2}} \\
&\times \left[ (1 - \cos \theta) \{\sin^2 \theta - (1 - \cos \theta)^2\}^{1/2} \cos \theta / \sin \theta - \{R^2 - r^2 (1 - \cos \theta)^2\}^{1/2} \sin \theta \right] \\
B^{\hat{\phi}} &= \frac{-B_0 R r (1 - \cos \theta)^2 \Omega_F \{\sin^2 \theta R^2 - r^2 (1 - \cos \theta)^4\}}{\sin \theta \{\sin^2 \theta R^2 - r^2 (1 - \cos \theta)^4\} \{R^2 - \Omega_F^2 r^4 (1 - \cos \theta)^4\}^{1/2}}, \tag{25}
\end{aligned}$$

where  $C$  and  $B_0$  represent the scale of field strength and  $R$  corresponds to the shape parameter for the hyperboloidal configuration. It is interesting to note that  $\Omega_F$  is an arbitrary function of  $r$  and  $\theta$ .

For the accretion flow, the magnetic field on the equatorial plane,  $\theta = \pi/2$ , is relevant. Among the accretion equations the implications of eq.(20) are quite different for those two configurations. For the hyperboloidal type,  $B^{\hat{r}} = 0$  on the equatorial plane in eq.(25) and eq.(20) reads

$$\Omega_D - \Omega_F = 0, \tag{26}$$

which may be considered to be the perfect-conductor boundary condition on the accretion disk. For the paraboloidal configuration, eq.(20) can be written as

$$\dot{M}_+ \frac{u^0}{u^r} (\partial_r u_\phi) [\Omega_D - \Omega_F] = -\frac{C^2}{4r(1 + \Omega_F^2)} (r^2 \Omega_F^2 - 1). \tag{27}$$

Hence one cannot expect  $\Omega_D = \Omega_F$  unless  $v_F (= r\Omega_F) = 1$  everywhere, which seems to be unphysical. It is natural to suppose that the velocity of the magnetic field line  $v_F (= r\Omega_F)$  does not exceed the speed of light. Then the r.h.s of the equation is positive. Since the term  $\dot{M}_+ (u^0/u^r) \partial_r u_\phi$  of the equation is negative, the term  $[\Omega_D - \Omega_F]$  has to be negative such that

$$\Omega_F > \Omega_D. \tag{28}$$

With a black hole at the center, however, the flat background is no more valid and the field configuration is expected to be changed accordingly. Since there is no known analytic solution in the background of a black hole, we have to rely on the numerical calculation. The detailed numerical calculation will be discussed in the next section particularly for the paraboloidal configuration in the Schwarzschild background.

In summary, we have a simple picture of accretion flow in an axisymmetric, stationary and force-free magnetosphere, which is described by the above four equations

in the frame work of a simplified two-dimensional disk model on the equatorial plane. The physical variables for this simple system[30] are  $u^0, u^r, u^\phi, \Psi, I$  and  $\dot{M}_+$ . Among those variables only  $\dot{M}_+$  is independent of the disk location and we take it as an input parameter in this work. Then we can solve the equations for this simple disk model to see the effect of the magnetic field on the accretion flow as well as to find the field configuration subject to the steady state accretion flow driven by the magnetic field itself.

### III. NUMERICAL RESULTS FOR A PARABOLOID-TYPE CONFIGURATION IN SCHWARZSCHILD BACKGROUND

In a flat background, we can find  $I$  and  $\Psi$  corresponding to the paraboloidal type configuration given by

$$I(X) = \frac{\pm C \Omega_F X}{2(1 + \Omega_F^2 X^2)^{1/2}}, \tag{29}$$

$$\frac{d\Psi}{dX} = \frac{\pi C}{(1 + \Omega_F^2 X^2)^{1/2}}, \tag{30}$$

where

$$X = r(1 \pm \cos \theta). \tag{31}$$

The explicit forms for the magnetic fields are just those given in the previous section, eq.(24). When  $\Omega_F$  is constant, we can easily integrate  $d\Psi/dX$  of eq.(30) to get explicit form of  $\Psi$  as

$$\Psi(X) = \frac{\pi C}{\Omega_F} \sinh^{-1}(\Omega_F X). \tag{32}$$

In the Schwarzschild background, the stream equation is given by

$$\begin{aligned} \partial_r \left\{ \left( 1 - \frac{2M}{r} \right) \partial_r \Psi \right\} + \frac{\sin \theta}{r^2} \partial_\theta \left( \frac{1}{\sin \theta} \partial_\theta \Psi \right) - \Omega_F \sin^2 \theta \partial_r (r^2 \Omega_F \partial_r \Psi) \\ - \frac{\Omega_F}{1 - \frac{2M}{r}} \sin \theta \partial_\theta (\sin \theta \Omega_F \partial_\theta \Psi) = - \frac{16\pi^2 I \frac{dI}{d\Psi}}{\left( 1 - \frac{2M}{r} \right)}. \end{aligned} \quad (33)$$

Compared to the case with flat background we do not have analytical forms like eq.(29) and (30). When  $\Omega_F$  and  $I$  are vanishing, eq.(33) becomes

$$\partial_r \left\{ \left( 1 - \frac{2M}{r} \right) \partial_r \Psi \right\} + \frac{\sin \theta}{r^2} \partial_\theta \left( \frac{1}{\sin \theta} \partial_\theta \Psi \right) = 0. \quad (34)$$

One of the solutions,  $\Psi_0$ , suggested by Blandford and Znajek [18] is given by

$$\Psi_0 = \pi C X, \quad (35)$$

where

$$X \equiv r(1 \mp \cos \theta) + 2M(1 \pm \cos \theta) \{1 - \log(1 \pm \cos \theta)\}, \quad (36)$$

and upper/lower sign refers to the upper/lower hemisphere. One can easily see that it reduces to the paraboloidal field lines for  $M \rightarrow 0$  or  $r \gg M$ . The upper (lower) sign corresponds to the northern (southern) hemisphere. It is interesting to note that the discontinuity of  $B^{\hat{r}}$  on the disk surface ( $\theta = \pi/2$ ) defines the toroidal surface current  $K^{\hat{\phi}}$

$$K^{\hat{\phi}} = \frac{C}{4\pi r}, \quad (37)$$

which is the same as in the flat background[2].

For non-vanishing  $\Omega_F$  and  $I$ , we consider a solution for which the shape of the magnetic surface are the same as

the magnetic surface defined by  $\Psi_0$ [22]. Thus  $\Psi, I$  and  $\Omega_F$  are assumed to depend on  $X$ . We suppose that the derivative of  $\Psi$  has the same form as in the flat background, eq.(30). That is, we take an Ansatz such that

$$\frac{d\Psi}{dX} = \frac{\pi C}{(1 + \Omega_F^2 X^2)^{1/2}}. \quad (38)$$

On the equatorial plane,  $X = r + 2M$ , we can construct magnetic fields on the disk surface as follows:

$$\begin{aligned} B^{\hat{r}} &= \frac{\pm C}{2r(1 + \Omega_F^2 X^2)^{1/2}}, \\ B^{\hat{\theta}} &= \frac{-C}{2r(1 + \Omega_F^2 X^2)^{1/2}} \left( 1 - \frac{2M}{r} \right)^{1/2}, \\ B^{\hat{\phi}} &= \frac{-2I}{r} \left( 1 - \frac{2M}{r} \right)^{-1/2}. \end{aligned} \quad (39)$$

Using eq.(38), eq.(33) can be written as

$$\frac{4\pi C \Omega_F}{(1 + \Omega_F^2 X^2)^{3/2}} \frac{\Delta}{(X - 2M)^2} = -16\pi^2 I \frac{dI}{d\Psi}, \quad (40)$$

where

$$\Delta = \frac{d\Omega_F}{dX} (X - 3M)(4M^3 - 6M^2 X + 5M X^2 - X^3) + \Omega_F \{10M^3 - 18M^2 X + 8M X^2 - X^3 + 3M^2 X(X - 2M)^2 \Omega_F^2\} \quad (41)$$

It can be considered to be an equation for  $I$  on the disk surface ( $\theta = \pi/2$ ) provided  $\Omega_F$  is given. In contrast to the flat background case, we do not have the analytic form for  $I$  analogous to eq.(29).

The accretion equations can then be written as follows,

$$(\partial_r u_0) \dot{M}_+ + \frac{C^2 \Omega_F}{(1 + \Omega_F^2 X^2)} \tilde{I} = 0, \quad (42)$$

$$(\partial_r u_\phi) \dot{M}_+ - \frac{C^2}{(1 + \Omega_F^2 X^2)} \tilde{I} = 0, \quad (43)$$

$$\dot{M}_+ \frac{u^0}{u^r} (\partial_r u_\phi) \left[ \frac{u^\phi}{u^0} - \Omega_F \right] + \frac{C^2}{4r(1 + \Omega_F^2 X^2)} \left( \frac{r^2 \Omega_F^2}{1 - \frac{2M}{r}} - 1 \right) = 0, \quad (44)$$

where a dimensionless quantity  $\tilde{I}$  for the upper hemisphere is defined by

$$\tilde{I} \equiv (1 + \Omega_F^2 X^2)^{1/2} \frac{I}{C}. \quad (45)$$

Four basic equations, eq.(40) - eq.(44), governing the accretion flow under the influence of paraboloidal-type

configuration are solved numerically[29]. We get the radial variations of  $u_0$ ,  $u_\phi$ ,  $I$  and  $\Omega_F$  on the disk with dimensionless variable  $\tilde{M}_+ = \dot{M}_+/C^2$  as an input parameter in this work. It should be noted that the dimensionless accretion rate parameter  $\tilde{M}_+$  is the relative magnitude of the accretion rate to  $C^2$  which determines the strength-squared of the magnetic field.

For numerical calculations, we need a set of initial values to start with. We take an initial point  $r_0$  far from the horizon such that we can make use of the Newtonian approach in the initial step of the numerical calculation. We take  $r_0$  to be much greater than inner most stable radius[23]

$$r_0 \gg 6M. \quad (46)$$

In this asymptotic region we can take initial values as those for the flat background approximation. At first, we choose initial values for  $u^0$  and  $u^\phi$  to be

$$u^0 = u_K^0, \quad u^\phi = \eta u_K^\phi, \quad (47)$$

where  $u_K^0$  and  $u_K^\phi$  are those for the Keplerian orbit. We take the initial value of  $u^\phi$  to be smaller than that of the Keplerian orbit to prevent  $u^r$  from becoming an imaginary number,  $\eta < 1$ . Plugging the initial values of  $u^0$  and  $u^\phi$  into eq.(43) and eq.(44), the initial value of  $\Omega_F$  can be determined. And the initial value of  $\tilde{I}$  is then determined by making use of flat-background relation in eq.(29):

$$\tilde{I} = \frac{1}{2}\Omega_F r. \quad (48)$$

After fixing these initial values, it is straightforward to execute the numerical calculation.

For numerical calculation, we consider two cases of the accretion-rate parameters, [a]  $\tilde{M}_+ = 0.7$  and [b]  $\tilde{M}_+ = 3$  and take initial point to be  $r_0 = 50M$ . To get some physical idea on the values of  $\tilde{M}_+$ , let us take  $C$  to be  $2.78 \times 10^{19}$  gauss-cm for a solar mass black hole as an example. Then the magnetic field strength becomes  $\sim 10^{12}$  gauss at  $r = r_0$  which might be compatible with the astrophysical phenomena accompanied with strong magnetic field, like magnetar and GRB [4]. Then the accretion rates are given by  $\dot{M}_+ = 1.8 \times 10^{28}$  g/s and  $7.7 \times 10^{28}$  g/s for  $\tilde{M}_+ = 0.7$  and 3 respectively.

We continue the numerical calculation inwardly up to  $r = 6M$  which is the radius of the innermost stable circular orbit in the Schwarzschild black hole at the center. As shown in Figure 1, the angular velocities of the magnetic field lines( $\Omega_F$ ) are found to be different from either the Keplerian angular velocity( $\Omega_K$ ) or the disk angular velocity( $\Omega_D$ ). It implies that the two-dimensional disk model may not be a good approximation for the accretion disk of perfect conductor. As expected in the previous section for the velocity of the magnetic field line  $v_F(= r\Omega_F)$  less than the speed of light,  $\Omega_F$  is found to be larger than  $\Omega_D$ .

For a smaller accretion rate,  $\tilde{M}_+ = 0.7$ ,  $\Omega_D$  changes its sign at  $r \sim 20M$  as shown in Figure 1[a]. It corresponds to changing its sense of rotation. It is because for a given strength of the magnetic field, the slope of angular momentum ( $\partial_r u_\phi$ ) is proportional to the inverse of  $\tilde{M}_+$  as can be seen in eq.(19). Hence the angular momentum of the accretion flow decreases more rapidly for smaller  $\tilde{M}_+$  and there is a chance of reverting the direction of rotation. But for larger  $\tilde{M}_+$ , the slope of change is not high enough to change the sense of rotation, Figure 1[b].

We obtain also the numerical solutions for  $\Psi$  and  $I$  of the stream equation to get the electromagnetic field on the disk. It is found that the strength of the magnetic field is increasing as  $r$  goes near the inner edge as shown in Figure 2. One can see that the axial component  $B^\phi$  is sensitive on  $\tilde{M}_+$  while  $B^r$  and  $B^\theta$  are not sensitive to  $\tilde{M}_+$ . The surface currents  $K^i$  are defined as discontinuities of the magnetic fields across the disk and they show similar behaviors as those of the magnetic field. Since the magnetic field as well as the surface current are increasing as  $r$  gets smaller, it is naturally expected that the Poynting flux increases substantially as  $r$  approaches to the center as shown in Figure 3. Although the numerical calculation does not go beyond  $r < 6M$ , it may indicate a possible electromagnetic jet structure near the inner edge of the disk.

#### IV. DISCUSSION

In this work, we investigate the accretion flow dominated by Poynting flux using a simplified model of a two-dimensional disk. The two-dimensional accretion disk in a force-free magnetosphere is described by the basic four equations, three accretion equations and one stream equation. We observe that the condition of the stationary accretion flow (constant  $\dot{M}_+$ ) gives rise to nontrivial constraints on the form of  $\Omega_F$  and on the configuration of the ambient electromagnetic field. It is found that it depends strongly on the types of field. In the flat background limit, we find that the hyperboloidal type configuration suggested by Blandford can accommodate the solutions with  $\Omega_F = \Omega_D$ , which is consistent with an accretion disk of perfect conductor. However for the paraboloidal type configuration,  $\Omega_F$  is expected to be greater than  $\Omega_D$ . Hence one can guess that a two-dimensional flow with paraboloidal type configuration might be relevant for an accretion disk not in a perfect-conducting state.

To get more details on the dynamics of the accretion flow, we try to find numerical solutions particularly for the paraboloidal type configuration in Schwarzschild background. The overall dynamics of the disk is found to depend essentially on the ratio of the accretion rate to the field strength-squared,  $\tilde{M}_+$ . When it is sufficiently small, the inner part of the accretion disk is found to be changing its sense of rotation to match the angular

momentum balance with respect to the Poynting flux.

One of the interesting results of this work is to demonstrate clearly how  $\Omega_F$  is different from either  $\Omega_D$  or  $\Omega_K$  under the influence of the strong magnetic field. Since the numerical calculation in this work is extended only up to the inner stable radius for the Schwarzschild black hole, the relativistic effect is found not to be dominant such that the discussion in a flat background limit does not change substantially. Hence the observation of  $\Omega_F = \Omega_D$  for hyperboloidal type configuration in a two-dimensional accretion flow is expected to be valid even with Schwarzschild black hole at the center.

We demonstrate in this work that how the accretion disk provides relevant boundary conditions, which is important to find the solutions of the stream equation. In this work it is possible basically because we have a mathematically well-defined disk surfaces in this simplified model as in the case of horizon. However it would be interesting to see whether any realistic accretion disk

model can provide the relevant boundary conditions for the stream equation, to which our analysis can be applied.

In order to simulate the strong relativistic effect it is necessary to extend the present study of the two-dimensional accretion flow to that in the Kerr background. However as the inner edge of the accretion disk gets very near/or beyond the ergo-sphere for a rapidly rotating black hole, the magnetic coupling between the black hole and the accretion disk[24, 25, 26] becomes important and the simple picture in this work should be modified substantially.

### Acknowledgments

This work was supported by the research fund of Hanyang University(HY-2003-1).

- 
- [1] R.V.E. Lovelace, *Nature* **262**, 649(1976)
  - [2] R.D. Blandford, *MNRAS* **176**, 465(1976)
  - [3] T. Piran, *Phys. Rep.* **314**, 575(1998)
  - [4] H.K. Lee, R.A.M.J. Wijers and G.E. Brown, *Phys. Rep.* **325**, 83(2000)
  - [5] H.K. Lee, G.E. Brown and R.A.M.J. Wijers, *ApJ* **536**, 416(2000)
  - [6] L.-X. Li, *Phys. Rev.* **D61**, 084016(2000)
  - [7] H.K. Lee and H.K. Kim, *J. Korean Phys. Soc.* **36**, 188(2000)
  - [8] L.-X. Li and B. Paczynski, *ApJ* **534**, L197(2000)
  - [9] P. Ghosh, *MNRAS* **315**, 89(2000)
  - [10] P. Ghosh and M.A. Abramowicz, *MNRAS* **292**, 887(1997)
  - [11] M. Livio, G.I. Ogilvie and J.E. Pringle, *ApJ* **512**, 100(1999)
  - [12] C. Fendt, *Astron. Astrophys.* **319**, 1025(1997)
  - [13] G.V. Ustyugova, R.V.E. Lovelace, M.M. Romanova, H. Li and S.A. Colgate, *ApJ* **541**, L21(2000)
  - [14] H. K. Lee, *Phys. Rev. D.*, **64**, 043006(2001); H. K. Lee, *J. Korean Phys. Soc.* **40**, 934(2002)
  - [15] T. Damour, *Phys. Rev. D* **18**, 3598(1978)
  - [16] K.S. Thorne, R.H. Price, and D.A. Macdonald, "Black Holes; The Membrane Paradigm" (Yale University Press, New Haven and London, 1986)
  - [17] M.A. Abramowicz, X.-M. Chen, M. Granath and J.-P. Lasota, *ApJ* **471**, 762(1996)
  - [18] R.D. Blandford and Z.L. Znajek, *MNRAS* **179**, 433(1977)
  - [19] V.S. Beskin, *Physics-Uspekhi*, **40**, 659(1997)
  - [20] D. Macdonald and K.S. Thorne. *MNRAS* **198**,345(1982)
  - [21] C. H. Lee, H. K. Lee and H. Kim, *J. Korean Phys. Soc.*, **43**, 24(2003)
  - [22] D. Macdonald, *MNRAS* **211**, 313(1984)
  - [23] S. Shapiro and S.A. Teukolsky, "Black Holes, White Dwarfs, and Neutron Stars" (John Wiley & Sons, New York, 1983)
  - [24] C.F. Gammie, *ApJ* **522**, L57(1999)
  - [25] J.H. Krolik, *ApJ* **515**, L73(1999)
  - [26] D.-X. Wang, W.-H. Lei and R.-Y. Ma, *MNRAS* **342**, 851(2003)
  - [27] M.C. Begelman, R.D. Blandford and M.J. Rees, *Rev. Mod. Phys.* **56**, 225(1984)
  - [28] H. K. Lee, in "Black Hole Astrophysics 2002", 6'th APCTP Winter School, Pohang, Korea, eds. H.K. Lee and M.G. Park (World Scientific, 2002)
  - [29] J. Park, MSc thesis, Hanyang University(2004)
  - [30]  $u^\theta = 0$  and only two of  $u^0, u^r, u^\phi$  are independent because of the velocity normalization,  $u^\mu u_\mu = -1$ .

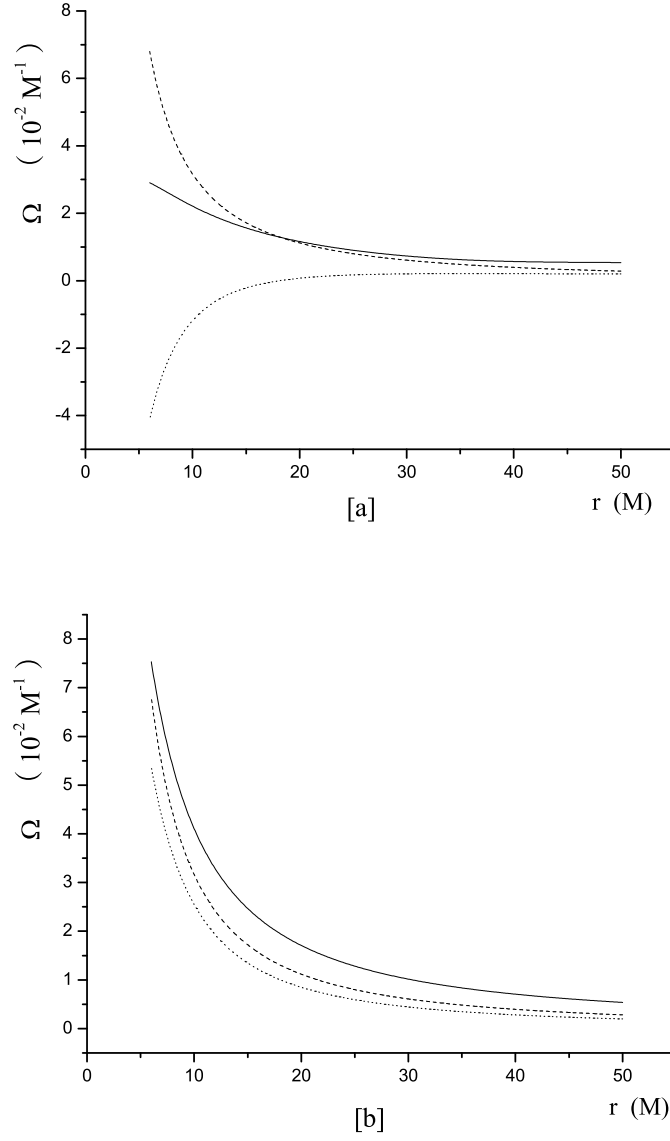


FIG. 1: The angular velocities of the magnetic surface  $\Omega_F$ , accretion disk  $\Omega_D$  and Keplerian orbit  $\Omega_K$  are shown in solid, dotted and dashed lines respectively for two cases of accretion rate: [a]  $\dot{M}_+ = 0.7$  and [b]  $\dot{M}_+ = 3$ .



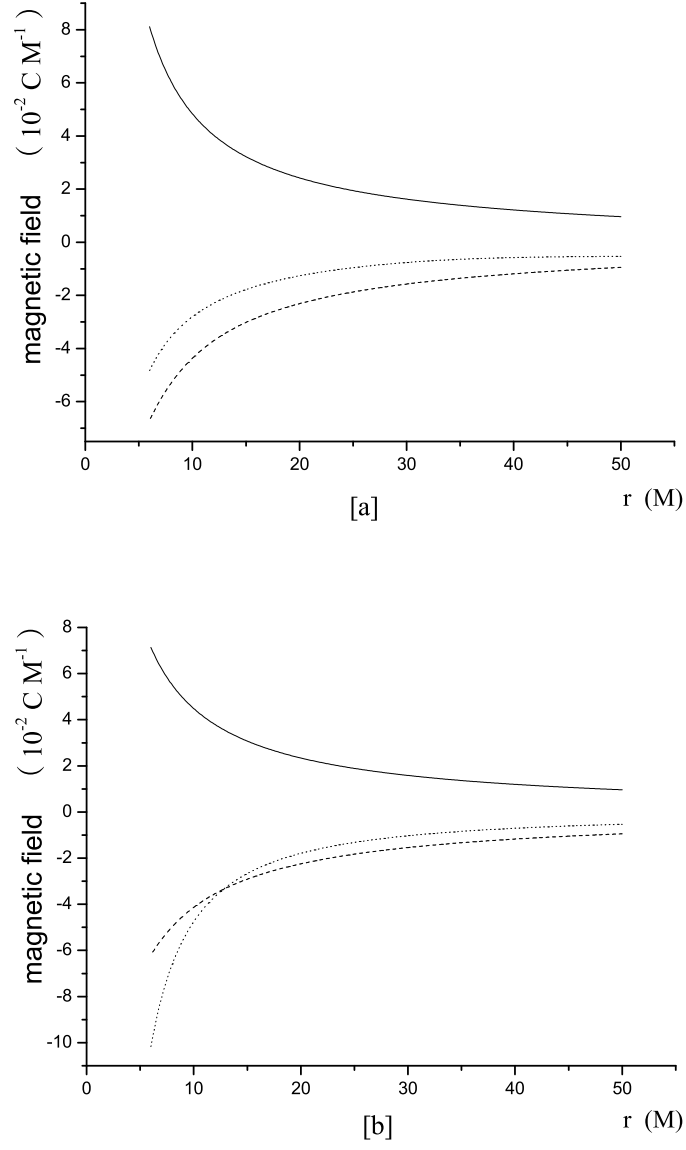


FIG. 2: The strength of the magnetic field in the upper hemisphere: the axial component  $B^{\hat{\phi}}$ ,  $B^{\hat{r}}$  and  $B^{\hat{\theta}}$  are represented by the dotted, solid and dashed lines respectively.

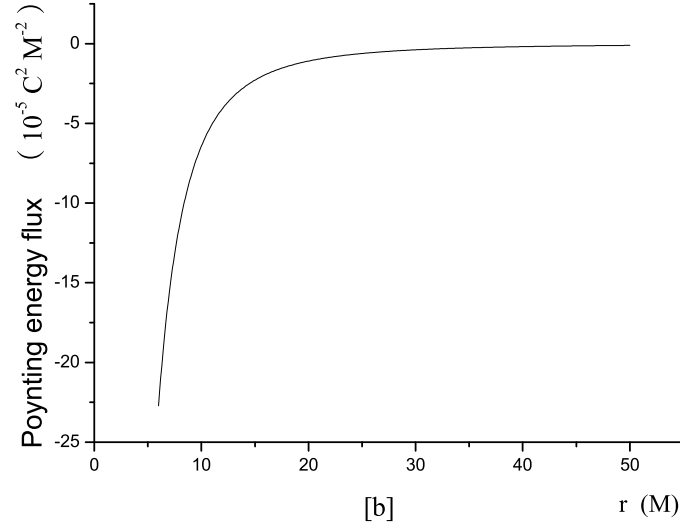
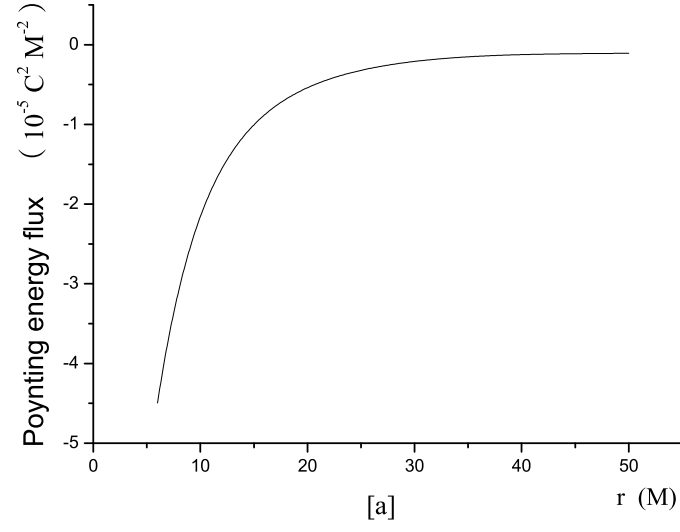


FIG. 3: Poynting energy flux,  $\mathcal{E}^{\hat{\theta}}$ , in the upper hemisphere.